Pure Appl. Chem., Vol. 81, No. 8, pp. 1459–1471, 2009.
doi:10.1351/PAC-CON-08-07-01

Microwaves and layered double hydroxides: A smooth understanding*

Patricia Benito, Francisco M. Labajos, and Vicente Rives‡

GIR-QUESCAT, Departamento de Química Inorgánica, Universidad de Salamanca, Salamanca, Spain

Abstract: Microwave-hydrothermal treatment (MWHT), a modification of conventional hydrothermal treatment, has been used during post-treatment of different layered double hydroxides (LDHs). In some cases, microwaves (MWs) have been used simultaneously with urea hydrolysis or for reconstruction of the LDH structure. The main advantages of replacing the conventional furnaces by MW ovens are a noticeable reduction in the time required to complete the process to obtain well-crystallized materials, and modification of their particle size distribution and textural and thermal properties. MW radiation leads to an increase in the rate of urea hydrolysis and consequently to fast precipitation of LDHs. Finally, the memory effect of Ni,Al-based LDHs is also improved.

Keywords: microwave radiation; hydrotalcite; layered double hydroxide; anionic clays; host–guest interactions.

INTRODUCTION

Layered double hydroxides (LDHs) having a hydrotalcite-like structure are formed by positively charged brucite-like layers, with charge-balancing anions and water molecules in the interlayers. They constitute the counterpart of the long-time known cationic clays. The most widely known LDHs contain M^{2+} and M^{3+} cations in the layers, but other systems containing M^{+}/M^{3+} or even M^{2+}/M^{4+} and $M^{2+}/M^{3+}/M^{4+}$ have been reported [1,2]. The nature of the layer cations can be changed among a wide possible selection almost exclusively restricted by charge and size (M^{2+} = Mg^{2+}, Ni^{2+}, Co^{2+}, Ni^{2+}, Zn^{2+}, etc.; M^{3+} = Al^{3+}, Cr^{3+}, Fe^{3+}, Rh^{3+}, V^{3+}, etc.), and the nature of the interlayer anion can be also (almost freely) selected, among organic and inorganic, simple or complex anions, polyoxometalates, simple anionic coordination compounds, biomolecules, etc. When calcined at moderate temperatures (450–600 °C), mixed oxides are obtained, and upon increasing the calcination temperature (up to 850 °C) metal oxide and spinel phases are segregated. The decomposition process takes place topotactically, and the solids obtained have small crystallite size, large specific surface area (100–300 $m^2\ g^{-1}$), and homogeneous and thermally stable interdispersion of the elements, which by reduction can lead to small and stable metal crystallites [3]. LDHs as prepared or after thermal treatment are promising materials for a large number of applications in catalysis, adsorption, medicine, photochemistry, electrochemistry, polymer chemistry, etc. All these properties are related to their high versatility, which can be achieved by modifying both their composition and synthesis method.

*Paper based on a presentation at the 8th Conference on Solid State Chemistry, 6–11 July 2008, Bratislava, Slovakia. Other presentations are published in this issue, pp. 1345–1534.

‡Corresponding author: vrives@usal.es

Coprecipitation is the synthesis method most widely applied [4]. It consists of precipitating a mixed hydroxide of both metal cations in the presence of a solution containing the anion to be hosted in the interlayer. Nucleation and particle growth overlap, and therefore differences in crystallinity over time and large crystallite size distributions are difficult to avoid. Up to now, aging constitutes the most widely used method to obtain well-crystallized, uniformly distributed particles. Post-treatment can be performed by vigorous stirring at moderate temperatures or by hydrothermal treatment to enhance both dissolution of the hydroxide precipitate and its subsequent crystal growth. However, achieving high crystallinity levels takes long periods of time (up to several days in some cases). Furthermore, segregation of some non-desired phases such as ZnO in Zn^{2+} containing LDHs [5] and the oxidation of Co^{2+} can also occur during the aging treatment [6].

On the other hand, the design of materials with improved technological requisites has led in the last years to the development of new synthetic routes, such as homogeneous precipitation using urea as precipitating agent [7–9]. On heating, urea releases ammonia and carbonate and a pH about 7–9, depending on the temperature, is reached. In this way, LDHs develop a better degree of crystallinity, forming particles fairly larger than those under conventional hydrothermal conditions, but with a narrower particle size distribution [10]. However, thermal activation of urea under atmospheric pressure takes a long time.

A well-known property of LDHs is their ability to recover the original lamellar structure after being calcined at moderate temperatures (400–600 °C) and then being exposed to water vapor, CO_2 or immersed in a solution containing different anions, the so-called "memory effect" [11]. The extent of the reconstruction depends on the precise nature of the layer cations, the temperature and time of calcination, and the number of cycles the LDH is calcined [11–13]. Usually, reconstruction is only observed for samples where the formation of well-crystallized materials (e.g., spinel) is avoided. Depending on the nature of the cations involved, total reconstruction requires different conditions and, for instance, severe conditions are needed for Ni,Al (NA) samples because of the segregation of spinel phases, i.e., only a partial reconstruction is achieved after hydrothermal treatment for long periods of time or even using high-temperature and -pressure conditions [14,15].

In order to reduce synthesis time, microwaves (MWs) can be used as a source of heating in the above-cited synthesis procedures. MWs are a portion of the electromagnetic spectrum with frequencies ranging from 300 MHz to 300 GHz. Their interaction with materials produces dipole reorientation in dielectric materials (dielectric heating) and ionic conduction if ions, which can be drift under the field, exist. In this way, it is possible to achieve a uniform bulk heating of the materials—volumetrically distributed heating—reducing thermal gradients usually found in conventional heating where energy is transferred by conduction, convection, or radiation from the surface of the vessel to the bulk of the material being heated. One of the most widely applications of the MW radiation is in hydrothermal processes, the so-called microwave-hydrothermal treatment (MWHT); the fast heating of the suspension or solution within the autoclave leads to significant advantages compared to high-pressure steel autoclaves used in conventional hydrothermal heating processes [16–18]. The temperature and pressure generated in such an autoclave depend on the level of input power, the dielectric loss of the reacting solution, the vapor pressure of the solvent, the volume of container occupied by the solvent, and whether or not gases are evolved during the reaction.

Since Komarneni and coworkers [19] reported in 1996 the use of MWHT during the synthesis of LDHs, several research teams have studied the application of MW radiation in the processing of LDHs [20–37]. All these authors agree on the considerable reduction in the synthesis time achieved by using MWs instead of conventional heating. Moreover, not only are the properties of the LDHs modified if treated under MW radiation, but also the properties of the oxides obtained after their thermal decomposition [27,29,38]. The enhanced crystallization was attributed to the formation of hot spots [19]. It was also reported that the MW coupling was due to the charged nature of the network and the water molecules existing in LDHs and that the enhancement depended on the precise nature of the trivalent cation [21]. However, some drawbacks were found by using MWs. Some authors re-

ported changes in the chemical composition of the compounds, such as lixiviation of aluminum cations from the layers of Mg,Al (MA) [20] and Ni,Mg,Al compounds [37]. Moreover, some concentration gradients from the bulk to the outer part of the particles were reported for Mg,Al compounds [31], and when Zn cations were involved a ZnO phase was always segregated, whichever the irradiation time used. Furthermore, the oxidation of LDHs containing Co^{2+} [24,26], and Mn^{2+} [34] was also accelerated. However, these works were performed under different conditions (domestic or laboratory MWs, open or closed vessels, different temperature and time) making it quite difficult to discern the actual effect of the MW radiation on the synthesis of LDHs in terms of MW interaction and characteristics of the synthesized materials.

In this work, we review our results obtained during the MW-assisted synthesis of LDHs, containing carbonate anions in the interlayer region, with different chemical compositions (Mg,Al; Mg,Cr; Ni,Al; Zn,Ni,Al; Zn,Al; Co,Al), but keeping the same synthesis conditions, in order to make proper comparisons. Specifically, MWHT was used to age samples obtained by coprecipitation [39–43], during homogeneous precipitation of LDHs using urea as precipitating agent [44,45] and in the reconstruction of NA compounds [46]. The MW method is proposed as a reliable alternative to conventional treatment. Rational discussion about the role of the MW radiation on properties of final solids will be given, together with the influence of the synthetic parameters (temperature and time) and the chemical composition of the LDHs.

EXPERIMENTAL

Microwave-hydrothermal treatment

MWHT was carried out in a Milestone Ethos Plus multimode cavity MW oven. Teflon digestion vessels, sealed and mounted on a turntable in the MW oven, were used. The temperature during the irradiation was continuously monitored with a thermocouple introduced in a reference vessel. The software dynamically controls the temperature profile, adjusting the power delivered at any time. The feedback mechanism optimizes the effects of too high temperature and pressure, and at the same time, prevents thermal runaways. In some experiments, solutions were kept under continuous stirring in MW vessels. The MW oven is equipped with an ASM-400 Magnetic Stirring Module device in the bottom of the MW cavity. An independently rotated magnet produces consistent stirring of solutions in all vessels, whichever their position within the cavity, when a stirring magnet bar is introduced in the vessels. For comparison purposes, conventional aging of the slurry was also performed at autogenous pressure in a stainless steel Phaxe 2000 bomb lined with Teflon. A volume of ca. 50 ml of solution per vessel was used in both MW and conventional procedures.

Synthesis of the solids

Coprecipitation

The slurry obtained by coprecipitation of an aqueous solution containing nitrates or chlorides of metal cations (Mg, Ni, Zn, Co, Al, and Cr) in desired amounts (M^{2+}/M^{3+} = 2/1) was mixed with an aqueous solution of Na_2CO_3 and NaOH at room temperature and submitted to MWHT at 125 °C (except for the Zn,Al–CO_3 series where two temperatures were tested, 100 and 125 °C) [39–43]. The duration of the treatment period was changed (from 10 to 300 min) to study the progress of crystallization under MW-hydrothermal conditions.

Urea method

A solution containing magnesium or nickel and aluminum chlorides (M^{2+}/Al^{3+} = 2/1) was mixed with urea to reach an urea/metal ions molar ratio of 3.3. The solution was placed in reaction vessels of the MW oven and heated at 100, 125, 150, or 175 °C for times ranging from 5 to 360 min, depending on the layer composition [44,45].

Reconstruction

Two series of Ni,Al–CO_3 compounds, with Ni^{2+}/Al^{3+} molar ratios 2 and 3, were synthesized by coprecipitation and submitted to MWHT for 300 min at 125 °C as reported in the Coprecipitation section above and calcined in air at 550 °C for 2 h (solids with molar ratio 2), or 450 and 550 °C for the solids with a Ni/Al molar ratio of 3. The reconstruction process was carried out at 100, 125, 150, or 175 °C for different periods of time by dispersing the oxides in a Na_2CO_3 aqueous solution, in distilled water and in a $NH_3 \cdot H_2O$ 10 wt % solution [46]. During the process, solutions were kept under continuous stirring in MW vessels.

Characterization techniques

Element chemical analysis for metal ions was carried out by atomic absorption in a Mark 2 ELL-240 apparatus, in Servicio General de Análisis Químico Aplicado (University of Salamanca, Spain). Powder X-ray diffraction (PXRD) patterns were recorded in a Siemens D-500 instrument using Cu-Kα radiation (λ = 1.54050 Å) and equipped with Diffrac AT software. Identification of the crystalline phases was made by comparison with the JCPDS files. Fourier transform-infrared (FT-IR) spectra were recorded in a Perkin–Elmer FT1730 instrument, using KBr pellets; 100 spectra (recorded with a nominal resolution of 4 cm^{-1}) were averaged to improve the signal-to-noise ratio. UV–vis spectra were recorded following the diffuse reflectance (UV–vis/DR) technique in a Perkin–Elmer Lambda 35 instrument with a Labsphere RSA-PE-20 integrating sphere and UV WinLab software, using 2-nm slits and MgO as a reference. Specific surface area assessment was carried out in a Gemini instrument from Micromeritics. The sample (ca. 80–100 mg) had been previously degassed in flowing nitrogen at 110 °C for 2 h in a FlowPrep 060 apparatus, also from Micromeritics, to remove physisorbed water. Data were analyzed using published software [47]. Transmission electron photographs were taken in Servicio General de Microscopía Electrónica (University of Salamanca, Spain) with a ZEISS-902 Microscope. Samples were dispersed in acetone by ultrasounds, and some drops of this suspension were deposited on a copper grid previously impregnated with an amorphous carbon film with a voltaic arc. Scanning electron photographs were recorded on a JEOL 6300 instrument at 25 kV in Universidad de Córdoba (Spain).

RESULTS AND DISCUSSION

Coprecipitated samples

The LDH structure is quite stable under the MW irradiation treatment. The chemical composition remained almost constant during MWHT, Table 1. Just a small decrease of the M^{2+}/M^{3+} is observed for all the series (except for NA and Zn,Al, ZA), as a consequence of the selective redisolution of the divalent cations and a preferential precipitation of the trivalent ones as a hydroxide, because of the larger acidity of the trivalent cations and the lower solubility of their hydroxides.

Table 1 Molar M^{2+}/M^{3+} ratios for the samples synthesized and submitted to different aging treatments (0: fresh sample; HW: MWHT treated for 10, 30, 60, 180, and 300 min; 3: conventional HT for 3 days).

Sample	MA	MC	NA	ZNA	ZA
0	1.93	1.90	2.24	2.09	2.13
HW10	1.91	1.88	2.24	2.12	2.23
HW30	1.91	1.69	2.22	2.06	2.23
HW60	1.91	1.82	2.20	2.01	2.16
HW180	1.91	1.82	2.22	2.00	2.23
HW300	1.87	1.85	2.24	1.95	2.25
3	2.01	1.91	2.22	2.09	–

MA: Mg,Al–CO_3; MC: Mg,Cr–CO_3; NA: Ni,Al–CO_3, ZNA: Zn,Ni,Al–CO_3; ZA: Zn,Al–CO_3

The main effect of MW heating is an enhancement of the crystallization rate of solids by improving the dissolution/recrystallization mechanism (Ostwald ripening), without the segregation of side phases (but Zn,Al, see below), Fig. 1. The improved order is achieved both in the stacking direction, (00*l*) diffraction peaks becoming sharper and more intense, and within the layers, as the (110) and (113) peaks are better resolved after long MWHT, whereas stacking faults (as evidenced by asymmetric diffraction maxima in the central region of the range studied) of the synthesized compounds are not removed. In the case of Zn,Al samples, when MW aging is performed at 125 °C, weak diffraction lines due to ZnO are recorded after 30 min treatment. Nevertheless, on decreasing the temperature to 100 °C, the patterns exclusively show the diffraction lines of pure Zn,Al–CO_3 compounds with narrow and symmetric diffraction lines. The results obtained can be explained by a uniform and fast heating of the slurry obtained by MWHT. Although the mechanism of interaction between the slurry and the MWs is not still clear, two different interactions can be proposed. First of all, the solvent is water, which is very receptive to commonly used MW frequencies. Moreover, the presence of "more active" water molecules [48], able to dissolve solids better than via thermal processes, could also enhance the Ostwald ripening process. Secondly, LDHs can be considered as efficient MW absorbers, since the charged nature of the network, the layer hydroxyl groups, and the presence of water and anions in the interlamellar region

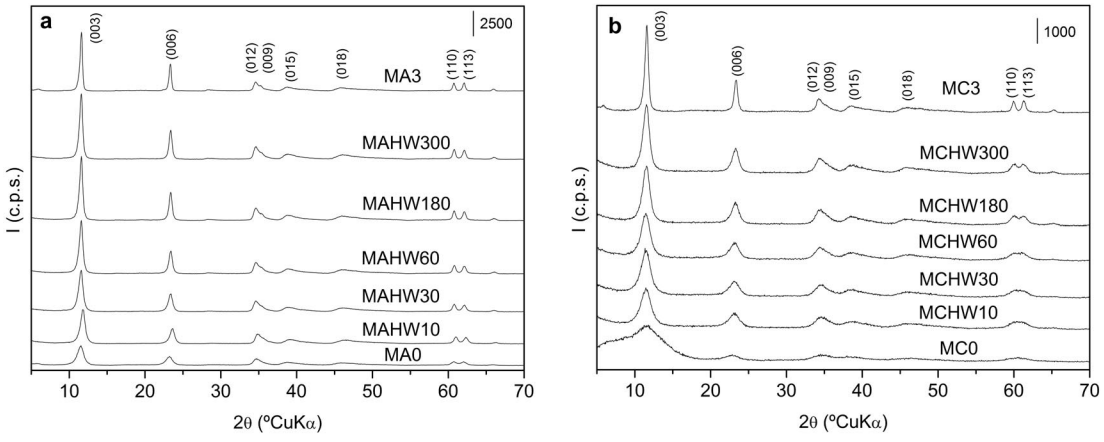

Fig. 1 PXRD patterns of coprecipitated samples (a: Mg,Al; b: Mg,Cr) fresh (0), submitted to MW-hydrothermal (MWHT for 10, 30, 60, 180, and 300 min) and conventional hydrothermal treatments (3: 3 days at 125 °C).

will favor the interaction with the electromagnetic field [21]. As a result of these interactions, the MW power needed to maintain the aging temperature in the vessels was only 100 W. Finally, "hot spots" could occur within the vessels, but it is not possible to measure them.

On comparing the "effectiveness" of MWHT on the enhancement of the crystallinity with respect to chemical composition, different behaviors are observed in the evolution of the PXRD patterns, Fig. 1, and in crystallite sizes of samples, as calculated in the (00*l*) stacking direction, see Table 2. The most noticeable enhancement at short periods of MWHT heating is observed for the Mg,Cr system, which preparation is not straightforward by coprecipitation. The fresh sample shows a rather diffuse PXRD pattern with broad reflections, but merely after 10 min the hydrotalcite-like structure is much better resolved. Conversely, the poorest improvement of crystallinity in comparison to the conventional process is found for Ni-containing samples, especially for the NA series. On the other hand, the best improvement at longer periods of time is observed for MA and Co,Al series, for which it seems that both conventional and MW aging lead to quite similar, well-ordered lamellar materials. The differences here observed could be related to the different crystallinity degree reached by the coprecipitated samples. But it is necessary to bear in mind that the interaction of a given material with MWs depends on dielectric properties of irradiated materials themselves and, on modifying the layer composition, dielectric properties may change as well.

Table 2 Crystallite sizes (nm) as calculated by the Scherrer equation averaging the values calculated when using the (003) and (006) diffraction planes. (0: fresh sample; HW: MWHT treated for 10, 30, 60, 180, and 300 min; 3: conventional HT for 3 days).

Sample	MA	MC	NA	ZNA	ZA
0	85	–	40	40	200
HW10	125	60	40	55	240
HW30	140	60	40	70	270
HW60	170	65	45	85	300
HW180	205	75	60	110	360
HW300	200	85	60	120	360
3	210	140	135	215	

MA: Mg,Al–CO_3; MC: Mg,Cr–CO_3; NA: Ni,Al–CO_3, ZNA: Zn,Ni,Al–CO_3; ZA: Zn,Al–CO_3

Results obtained by PXRD are confirmed by FT-IR spectroscopy, Fig. 2. The shape of infrared bands was modified along the treatment. As a result of strong layer–interlayer interactions and a better ordered interlayer region on increasing the irradiation time, the ν(OH) band at 3460–3400 cm^{-1} becomes more symmetric and the shoulder around 2900 cm^{-1} ascribed to the bridging mode H_2O–CO_3^{2-} is more intense. This fact is more pronounced for Ni,Al, Zn,Ni,Al, Co,Al, and Zn,Al samples. Moreover, the antisymmetric $\nu_3(CO_3^{2-})$ mode at ca. 1358 cm^{-1}, recorded as a broad and nonsymmetric peak for low-crystalline samples due to the decrease of the symmetry of the anion, becomes narrower upon increasing the treatment time, suggesting a weaker perturbation of the CO_3^{2-} symmetry inside the interlayer. Finally, the overlapped bands recorded in the low wavenumber region, ascribed to lattice vibrations, are more intense and better-resolved for treated samples than for the starting materials. Narrowing of bands is probably due to an increase in cation ordering.

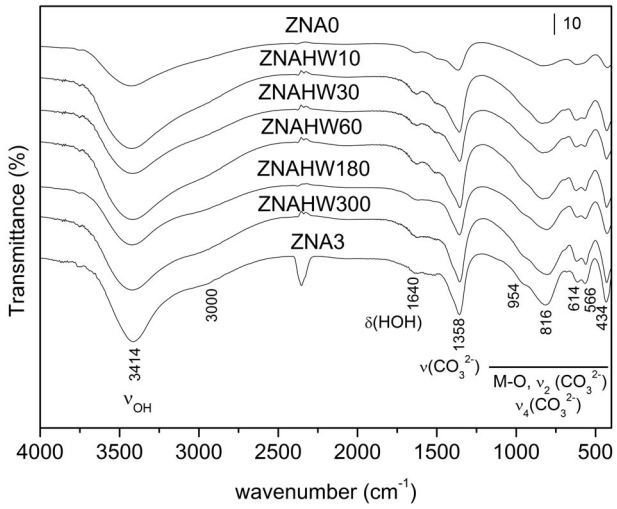

Fig. 2 FT-IR spectra of Zn,Ni,Al (ZNA) samples obtained by coprecipitation, nontreated (0) and aged under MWHT (10, 30, 60, 180, and 300 min) and conventional treatment (3: 3 days at 125 °C) .

UV–vis spectroscopy confirms that the immediate environment of the cations Ni^{2+}, Cr^{3+}, and Co^{2+} in the layers is not modified with MWHT. Furthermore, it confirms that no partial oxidation of Co^{2+} to Co^{3+} takes place under MWHT conditions, while it readily happens under conventional aging.

Textural properties of LDHs can also be modulated using MWs. MWHT leads to a narrowing of the hysteresis loops related to a progressive cancellation of interparticle pores. Two trends are observed in the S_{BET} values (Table 3) depending on series (pore volumes follow the same trend, with the exception of Mg,Cr samples). On one hand, an increase is observed when the slurry is heated under MW field for short irradiation times. After this increase, a decrease in the values is observed when submitting the sample to longer treatment periods, except for Mg,Cr samples, where specific surface area remains almost constant whichever the irradiation time. In all cases, the surface area of samples irradiated for 300 min is larger than that measured for the sample aged by conventional hydrothermal treatment. On the other hand, a decrease occurs for Zn,Al and Co,Al series when the slurry is aged under MW radiation, and even a cancellation of the measured values is observed for Zn,Al samples. Taking into account that using nitrogen as adsorbate only the external surface area is measured (the nitrogen molecules cannot access to the interlayer space, populated by carbonate anions and water molecules), and that pore volume and hysteresis loops correspond to interparticle pores, the differences observed here should arise from a modification of the morphology of the particles (size, shape, and distribution). In poor crystalline samples, small particles are aggregated, decreasing the total external area, a fact clearly observed in the Mg,Cr system where the fresh MC0 sample shows no measurable specific surface area. Assuming the dissolution–reprecipitation process, a simultaneous precipitation of many nuclei occurs during aging at short times, giving rise to a higher surface area/volume unit ratio. On increasing the irradiation time, the crystal growth and defect removal yield to a decrease of the S_{BET} and interparticle pores.

Table 3 Specific surface area (S_{BET} m^2 g^{-1}) for samples of different series aged under MW (MWHT for 10, 30, 60, 180, and 300 min at 125 °C, for ZA at 100 °C) and conventional treatment (3 days at 125 °C).

Sample	MA	MC	NA	ZNA	ZA
0	60	nd	51	23	40
HW10	85	122	175	61	35
HW30	81	141	172	88	23
HW60	75	155	169	104	18
HW180	64	154	151	88	15
HW300	59	153	144	70	nd
3	22	87	76	44	

MA: Mg,Al–CO_3; MC: Mg,Cr–CO_3; NA: Ni,Al–CO_3, ZNA: Zn,Ni,Al–CO_3; ZA: Zn,Al–CO_3

Transmission electron microscopy images agree with the above hypothesis. For fresh samples, even after extensive dispersion, agglomeration of particles is observed. After short irradiation times, a homogeneous particle size distribution is obtained although no change in the shape of the particles is observed. However, evolution of particle shape is also dependent on its chemical composition. Moreover, MW-assisted prepared solids are constituted by smaller particles with similar sizes, whereas conventionally treated samples are formed by bigger particles with different sizes. These differences are explained on the basis of thermal gradients taking place within the autoclave in the conventional method, which are avoided when using the MW treatment. A simultaneous fast dissolution of the gel increases supersaturation, and a short and abundant nucleation period would favor a larger number of smaller particles with a narrower particle size distribution. On the other hand, growing of particles under conventional heating takes place following temperature gradients by dissolution and precipitation of the particles, leading to formation of more perfect as well as larger crystallites (Ostwald ripening), but with a broader particle size distribution.

Urea method

The urea method coupled to MWHT leads to a faster formation of the LDH structure than with conventional hydrothermal treatment. For instance, for MA samples at 150 °C, a pure LDH compound was obtained in 30 min, whereas a 5-h treatment is required in the conventional method to reach samples with similar PXRD patterns using the same oven temperature. In the former method, volumetric heating promotes a faster urea hydrolysis. Contrarily, in the latter method a short treatment time is probably not enough to achieve the set temperature within the reactor and temperature gradients are generated within the autoclave.

Some differences are observed during formation of the LDH structure depending on the nature of divalent cations existing in the layers. A pseudo-boehmite phase is formed at short times for MA samples and then magnesium cations are incorporated in the structure, while the only crystalline phase recorded in NA samples is the hydrotalcite one, Fig. 3. Once the hydrotalcite phase precipitates, similarly to coprecipitated samples, an increase in irradiation time yields to an enhancement of crystallinity in MA series forming well-crystallized compounds without staking defaults. Nevertheless, no appreciable effect of the treatment on crystallinity is observed for NA compounds even though the time is extended (up to 360 min) and the temperature increased (up to 175° C). Moreover, conventional treatment for long time (24 h) yields to better-crystallized compounds.

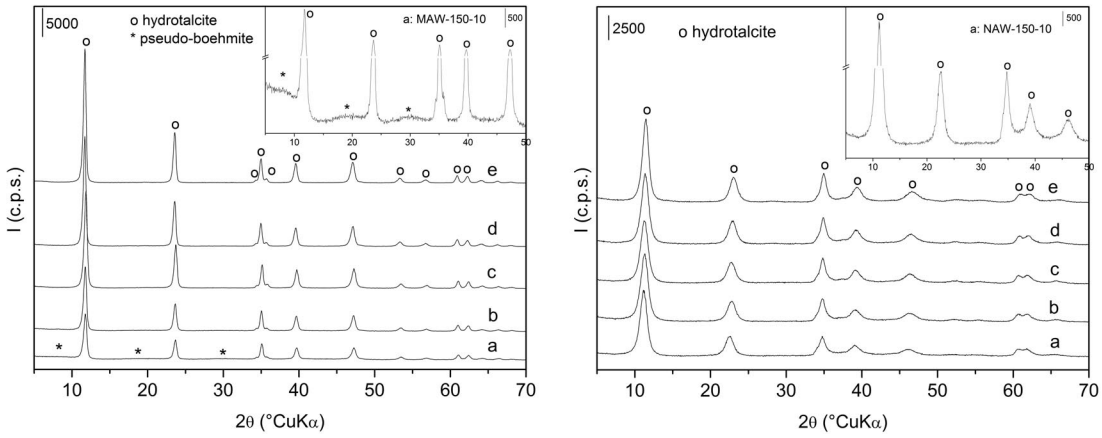

Fig. 3 PXRD patterns of MA, left, and NA, right, samples obtained by the MW-assisted urea hydrolysis method at 150 °C and increasing periods of MWHT (a: 10, b: 20, c: 30, d: 60 and e: 120 min).

The differences observed between NA and MA samples must be related to the pH required to obtain the LDH, lower for NA samples [49]. Thus, this value is more easily reached in the experiments here reported, making it impossible to observe the first steps of the growing mechanism.

The behavior of interlayer anions in LDHs under MW irradiation depends on their chemical composition. FT-IR spectroscopy, Fig. 4, shows that carbonates are steadily incorporated into the structure of MA samples with increasing radiation time. But for Ni-containing samples, together with carbonates, some cyanate anions, an intermediate product of the urea hydrolysis, are incorporated into the structure [50], as confirmed by the presence of a new band at ca. 2180 cm^{-1} due to the C–N stretching mode of cyanate anions in the interlayer, and the [$\delta(OCN^-)$] mode is also recorded at ca. 620 cm^{-1}. CNO^- species are steadily released during the synthesis with the concomitant inclusion of carbonates, also confirmed by element chemical analyses. They could not be completely removed despite the severe synthesis conditions (long irradiation times and high temperatures) that were applied. On the other hand, the characteristic spectrum of LDH intercalated with carbonate is obtained after 12 and 24 h of conventional hydrothermal treatment; moreover, the best resolution of the lattice M–O bands points to an improvement of the crystallinity for these samples. The release of cyanate species is also

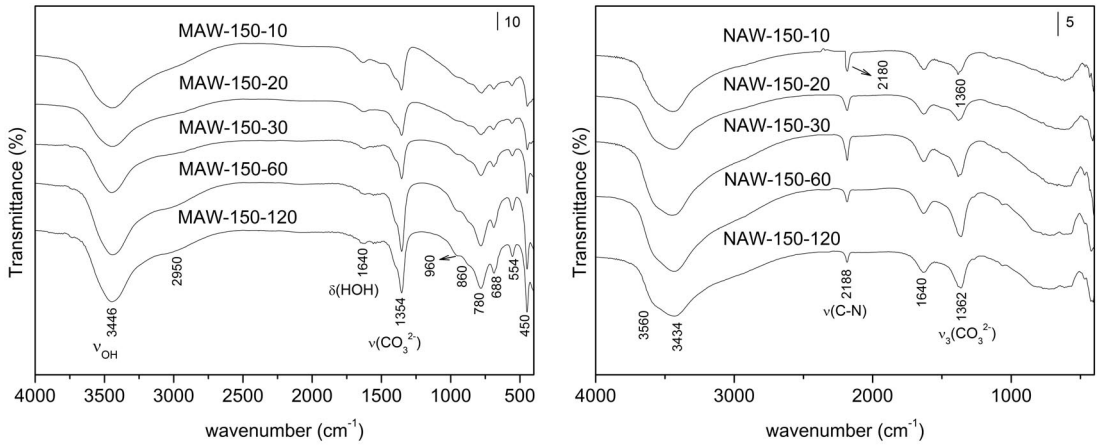

Fig. 4 FT-IR spectra of MA, left, and NA, right, samples prepared by the MW-assisted urea method at 150 °C.

accompanied by a decrease in the Ni/Al ratio in the solid, because of the formation of soluble $[Ni(NH_3)_6]^{2+}$ complexes.

In agreement with the results obtained by PXRD, the morphological properties (S_{BET}, pore size distribution, and particle size and shape) are also dependent on the synthesis conditions and the chemical composition, Table 4. MA samples prepared at short irradiation times show large specific surface areas due to the presence of the amorphous alumina phase, and a decrease in the S_{BET} is observed on increasing both the time and temperature. Conversely, after an increase of the surface after 20 min, almost constant values were obtained for NA samples.

Table 4 Specific surface area values (S_{BET}, $m^2\ g^{-1}$) of samples prepared by MW-assisted method at increasing periods of time (MWHT for 10, 20, 30, 60, and 120 min).

Sample	MA	NA
HW10	106	54
HW20	73	85
HW30	40	74
HW60	24	87
HW120	21	80

MA: Mg,Al–CO_3; NA: Ni,Al–CO_3

Scanning electron microscope (SEM) images of Mg-containing samples prepared at 150 °C show that well-defined hexagonal particles with a homogeneous particle size distribution are obtained, Fig. 5, left. On the other hand, NA particles form aggregates constituted by smaller particles, Fig. 5, right. Hydrolysis of urea gives rise to a slow pH increase, i.e., low supersaturation, leading to a slow nucleation process and favoring the crystal growth. However, since MW radiation leads to a fast increase in urea hydrolysis all over the vessel, a uniform growth environment is attained and the supersaturation can be increased, favoring a fast nucleation, giving rise to a larger number of nuclei which produce a larger number of small crystals of uniform size. In the case of NA samples, the anomalous behavior observed could be explained in terms of cyanate intercalation with the formation of an interstratified phase, which could inhibit the growing process.

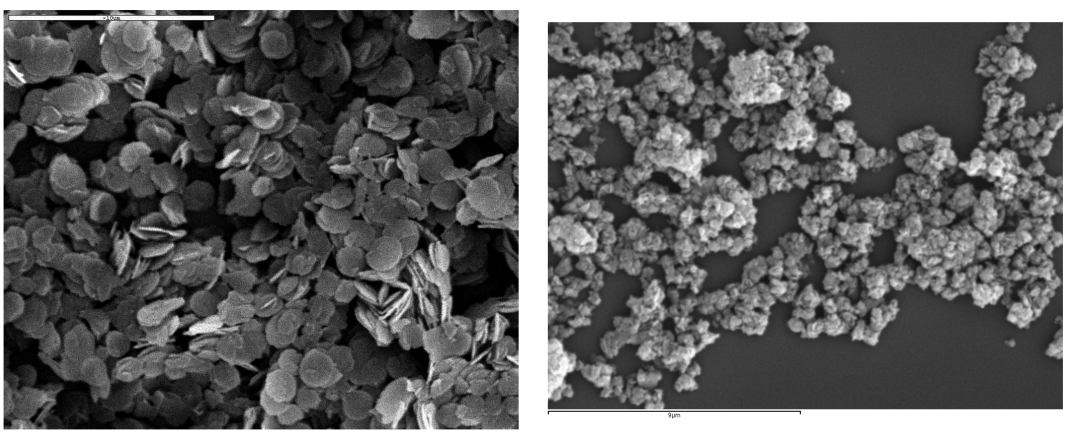

Fig. 5 SEM images of samples prepared by the MW-assisted urea method at 150 °C for 60 min (left: MA; right: NA).

Memory effect

Full reconstruction of the hydrotalcite-like structure from mixed oxides obtained by calcination of NA compounds at 550 °C can be easily achieved in a carbonate-containing solution, Fig. 6. When the process is performed at 125 °C, diffraction patterns show that lamellar structure starts to appear in the first 10 min, but it is necessary to extend the treatment up to 300 min to obtain a single LDH phase. These results agree with those obtained by UV–vis spectroscopy [46], more sensitive to local environment of Ni^{2+} species, confirming that all Ni^{2+} species are located in octahedral positions within the hydroxyl layers. Reconstruction time also depends on temperature: while at 125 °C a 300-min treatment is required to fully recover the original lamellar structure, on increasing temperature synthesis time is reduced (180 and 60 min at 150 and 175 °C, respectively) [46]. Finally, it should be noticed that reconstructed solids show improved crystallinity in comparison with the precursor (Ni,Al–CO_3 LDH coprecipitated and submitted to MWHT at 125 °C for 300 min); the crystallite size calculated from the Scherrer's equation is 60 nm for the precursor while 120 nm for the reconstructed sample.

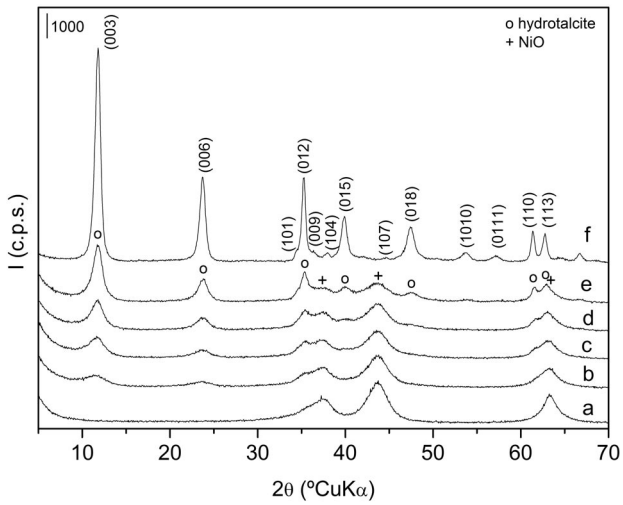

Fig. 6 Evolution of the structure of the solids during the MW-assisted reconstruction (a: calcined sample, b,c,d,e,f: samples reconstructed at 125 °C for 10, 30, 60, 180 and 300 min, respectively).

The higher crystallinity of the reconstructed materials can be related to two facts. If a topotactic reconstruction process is assumed, the memory effect would lead to a larger degree of crystallinity, compared to that imparted on the LDH prepared by coprecipitation, because of cations that are still homogeneously distributed in the mixed oxides. However, the enhancement could be also related to an increase in crystallinity during the MW treatment, similar to that observed during aging treatment of coprecipitated samples (Ostwald ripening).

In an attempt to obtain NA compounds intercalated with hydroxyl anions, reconstruction was also performed in distilled water. However, despite the modification of reconstruction parameters (time and temperature) and decreasing calcination temperature (450 °C), no successful results were obtained. Moreover, segregation of Al-containing phases (bayerite and boehmite) was observed during the reconstruction process [46]. Although the reconstruction degree was increased and segregation of Al phases was avoided by replacing distilled water by an ammonia aqueous solution, no full reconstruction was achieved either.

Assuming a dissolution–precipitation mechanism for the reconstruction process, the poorly crystalline oxide gives rise to a concentrated solution of reactive species from which LDH precipitates. MW

radiation improves the dissolution process of the oxide or hydroxide phases, a behavior that can be related to the formation of "active water molecules" as explained in the Urea method section [48]. It could also enhance formation of nucleation sites; on the other hand, as MW radiation is able to increase the mobility of ions formed it might improve as well diffusion of species to nucleation sites. However, the pH must be high enough to dissolve the phases.

CONCLUSIONS

MWHT makes it possible to prepare LDHs with improved properties, such as small and homogeneous particle size distribution, enhanced crystallinity, and larger specific surface areas, in comparison to conventional hydrothermal treatment. This constitutes a reliable alternative to conventional hydrothermal treatment, allowing us to overcome some drawbacks observed in conventional synthesis of several systems, such as Mg,Cr, Zn,Al, and Co,Al; to reduce synthesis time when urea is used as precipitation agent; and also complete reconstruction of the lamellar structure of some mixed oxides obtained upon calcination of NA compounds, which otherwise requires severe conditions with conventional methods. It can be stated that a thermal effect, i.e., volumetric heating, is the main responsible for the reduction of synthesis time and properties of the solids obtained, as it improves the dissolution–reprecipitation processes. It has been shown that the Ostwald ripening mechanism, responsible for growth of crystals, can be improved, and homogeneous heating of all the solution leads to smaller-sized and more homogeneous compounds.

ACKNOWLEDGMENTS

The authors thank Dr. Cristobalina Barriga for her assistance in obtaining SEM images. PB acknowledges a grant from JCyL. The authors thank ERDF and MEC (Grant MAT2006-10800-C02-01) for financial support.

REFERENCES

1. V. Rives. In *Layered Double Hydroxides: Present and Future*, V. Rives (Ed.), Nova Science Publishers, New York (2001).
2. X. Duan, D. G. Evans. In *Layered Double Hydroxides*, **119** (2006).
3. F. Basile, A. Vaccari. In *Layered Double Hydroxides: Present and Future*, V. Rives (Ed.), pp. 285–321, Nova Science Publishers, New York (2001).
4. W. Reichle. *Solid State Ionics* **22**, 135 (1986).
5. J. T. Kloprogge, L. Hickey, R. L. Frost. *J. Solid State Chem.* **177**, 4047 (2004).
6. M. A. Ulibarri, J. M. Fernández, F. M. Labajos, V. Rives. *Chem. Mater.* **3**, 626 (1991).
7. U. Costantino, F. Marmottini, M. Nocchetti, R. Vivani. *Eur. J. Inorg. Chem.* **10**, 1439 (1998).
8. M. Ogawa, H. Kaiho. *Langmuir* **18**, 4240 (2002).
9. M. Adachi-Pagano, C. Forano, J.-P. Besse. *J. Mater. Chem.* **13**, 1988 (2003).
10. J.-M. Oh, S.-H. Hwang, J.-H. Choy. *Solid State Ionics* **151**, 285 (2002).
11. T. Sato, H. Fujita, T. Endo, M. Shimada, A. Tsunashima. *React. Solids* **5**, 219 (1988).
12. T. Hibino, A. Tsunashima. *Chem. Mater.* **10**, 4055 (1998).
13. J. Rocha, M. del Arco, V. Rives, M. A. Ulibarri. *J. Mater. Chem.* **9**, 2499 (1999).
14. B. Rebours, J. B. d'Espinose de la Caillerie, O. Clause. *J. Am. Chem. Soc.* **116**, 1707 (1994).
15. F. Prinetto, G. Ghiotti, P. Graffin, D. Tichit. *Microporous Mesoporous Mater.* **39**, 229 (2000).
16. S. Komarneni, V. C. Menon. *Mater. Lett.* **27**, 313 (1996).
17. N. Kumuda, N. Kinomura, S. Komarneni. *Mater. Res. Bull.* **33**, 1411 (1998).
18. H. Katsuki, S. Furuta, S. Komarneni. *J. Am. Ceram. Soc.* **82**, 2257 (1999).
19. S. Komarneni, Q. H. Li, R. Roy. *J. Mater. Res.* **11**, 1866 (1996).

20. G. Fetter, F. Hernández, A. M. Maubert, V. H. Lara, P. Bosch. *J. Porous Mater.* **4**, 27 (1997).
21. S. Kannan, R. V. Jasra. *J. Mater. Chem.* **10**, 2311 (2000).
22. G. Fetter, M. T. Olguin, P. Bosch, S. Bulbulian. *J. Porous Mater.* **7**, 469 (2000).
23. G. Fetter, A. Botello, V. H. Lara, P. Bosch. *J. Porous Mater.* **8**, 227 (2001).
24. B. Zapata, P. Bosch, G. Fetter, M. A. Valenzuela, J. Navarrete, V. H. Lara. *Int. J. Inorg. Mater.* **3**, 23 (2001).
25. S. Möhmel, I. Kurzawski, D. Uecker, D. Müller, W. Gebner. *Cryst. Res. Technol.* **37**, 359 (2002).
26. B. Zapata, P. Bosch, M. A. Valenzuela, G. Fetter, S. O. Flores, I. R. Córdova. *Mater. Lett.* **57**, 679 (2002).
27. D. Tichit, A. Rolland, F. Prinetto, G. Fetter, M. J. Martínez-Ortiz, M. A. Valenzuela, P. Bosch. *J. Mater. Chem.* **12**, 3832 (2002).
28. M. Z. bin Hussein, Z. Zainal, A. H. Yahaya, D. W. V. Foo. *J. Mater. Syn. Proc.* **2**, 89 (2002).
29. M. J. Climent, A. Corma, S. Iborra, K. Epping, A. Velty. *J. Catal.* **225**, 316 (2004).
30. C. Chen, C. Xu, L. Feng, Z. Li, J. Suo, F. Qiu, Y. Yang. *Adv. Synth. Catal.* **347**, 1848 (2005).
31. J. A. Rivera, G. Fetter, P. Bosch. *Microporous Mesoporous Mater.* **89**, 306 (2006).
32. S. P. Paredes, G. Fetter, P. Bosch, S. Bulbulian. *J. Mater. Sci.* **41**, 3377 (2006).
33. S. P. Paredes, G. Fetter, P. Bosch, S. Bulbulian. *J. Nucl. Mater.* **359**, 151 (2006).
34. A. Sampieri, G. Fetter, H. Pfeiffer, P. Bosch. *Solid State Sci.* **9**, 394 (2007).
35. M. Jobbagy, M. A. Blesa, A. E. Regazzoni. *J. Colloid Interface Sci.* **309**, 72 (2007).
36. J. A. Rivera, G. Fetter, Y. Jimenez, M. X. Xochipa, P. Bosch. *Appl. Catal., A* **316**, 207 (2007).
37. O. Bergada, I. Vicente, P. Salagre, Y. Cesteros, F. Medina, J. E. Sueiras. *Microporous Mesoporous Mater.* **101**, 363 (2007).
38. F. Basile, P. Benito, G. Fornasari, F. M. Labajos, V. Rives, A. Vaccari. *Stud. Surf. Sci.* **162**, 761 (2006).
39. P. Benito, F. M. Labajos, J. Rocha, V. Rives. *Microporous Mesoporous Mater.* **94**, 148 (2006).
40. P. Benito, F. M. Labajos, V. Rives. *J. Solid State Chem.* **179**, 3784 (2006).
41. M. Herrero, P. Benito, F. M. Labajos, V. Rives. *J. Solid State Chem.* **180**, 873 (2007).
42. M. Herrero, P. Benito, F. M. Labajos, V. Rives. *Catal. Today* **128**, 129 (2007).
43. P. Benito, I. Guinea, F. M. Labajos, J. Rocha, V. Rives. *Microporous Mesoporous Mater.* **110**, 292 (2008).
44. P. Benito, F. M. Labajos, V. Rives. *Cryst. Growth Des.* **6**, 1961 (2006).
45. P. Benito, M. Herrero, C. Barriga, F. M. Labajos, V. Rives. *Inorg. Chem.* **47**, 5453 (2008).
46. P. Benito, I. Guinea, F. M. Labajos, V. Rives. *J. Solid State Chem.* **181**, 987 (2008).
47. V. Rives. *Adsorption Sci. Technol.* **8**, 95 (1991).
48. M. C. R. Symons. *Acc. Chem. Res.* **14**, 179 (1981).
49. J. Boclair, P. Braterman. *Chem. Mater.* **11**, 298 (1999).
50. B. Mavis, M. Akinc. *Chem. Mater.* **18**, 5317 (2006).